This is a repository copy of *Quantifying the effect of particle characteristics on wheel/rail adhesion & damage through high pressure torsion testing*.

White Rose Research Online URL for this paper:
https://eprints.whiterose.ac.uk/194806/

Version: Published Version

Article:
Skipper, W.A. orcid.org/0000-0001-8315-2656, Nadimi, S., Watson, M. et al. (2 more authors) (2023) Quantifying the effect of particle characteristics on wheel/rail adhesion & damage through high pressure torsion testing. Tribology International, 179. 108190. ISSN 0301-679X

https://doi.org/10.1016/j.triboint.2022.108190

Reuse
This article is distributed under the terms of the Creative Commons Attribution (CC BY) licence. This licence allows you to distribute, remix, tweak, and build upon the work, even commercially, as long as you credit the authors for the original work. More information and the full terms of the licence here: https://creativecommons.org/licenses/

Takedown
If you consider content in White Rose Research Online to be in breach of UK law, please notify us by emailing eprints@whiterose.ac.uk including the URL of the record and the reason for the withdrawal request.

eprints@whiterose.ac.uk
https://eprints.whiterose.ac.uk/

Tribology International 179 (2023) 108190

Contents lists available at ScienceDirect

Tribology International

journal homepage: www.elsevier.com/locate/triboint

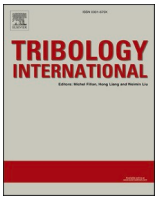

Quantifying the effect of particle characteristics on wheel/rail adhesion & damage through high pressure torsion testing

W.A. Skipper [a,*], S. Nadimi [b], M. Watson [a], A. Chalisey [c], R. Lewis [a]

[a] Leonardo Centre for Tribology, The University of Sheffield, Sheffield, United Kingdom
[b] School of Engineering, Newcastle University, Newcastle upon Tyne, United Kingdom
[c] RSSB, The Helicon, One South Place, London, United Kingdom

ARTICLE INFO

Keywords:
Wheel/rail contact
Friction
Sanding
Leaves on the line

ABSTRACT

Low adhesion in the wheel/rail contact is a problem for the rail industry in Great Britain as it causes significant scheduling and safety issues. Applying sand to the wheel/rail contact is used to mitigate against low adhesion however, there is not a consensus on what makes a "good" particle for restoring adhesion, especially with regards to when the particle has entered the wheel/rail contact. The aim of this work was to investigate what particle characteristics had the greatest effect on wheel/rail adhesion and surface conditions, using a process of particle characterisation, tribological testing and statistical modelling. Particle size, shape, and hardness were all found to affect tribological performance. This knowledge can help guide future changes to sanding operations.

1. Introduction

1.1. Background

Low adhesion[1] within the wheel/rail contact of a train is estimated to cost the British rail industry ~£345 m/annum [1]; the loss of traction when accelerating and braking can lead to timetable delays [2] and safety issues (e.g. signals passed at danger or in the worst case collisions [3]) respectively. Low adhesion conditions can be created by the contaminants in the wheel/rail contact, such as: oils [4], water [5], wetted oxides [6], and leaves on the line [7].

Sanding has been used for increasing adhesion in the wheel/rail contact for centuries in the UK. Typically, dry sand particles are applied via an air stream directed at the contact [8]. Particles can also be applied to the wheel/rail contact within a gel, these are generally called friction modifiers (FM) [2]. These are typically applied using track-side applicators, applying FM directly onto the rail head via a pumping system. These can also be applied using train-borne applicators.

Whilst the application of particles to increase traction has long been used, there is currently little consensus on what makes a "good" sand for increasing traction in the wheel/rail contact, or whether sand particles are necessarily the best type of particle for mitigating low adhesion. In addition, minimising any possible negative effects from the application of adhesion restoring particles is also important when deciding how well a particle performs, e.g. wheel/rail damage, or a loss of train detection. Full reviews concerning previous work on this topic, and the identified knowledge gaps remaining, have previously been published to this effect [9,10].

In this paper, an investigation has been conducted to determine what characteristics of a particle have an effect on tribological performance, and to what extent, under a variety of different test conditions. To achieve this a range of particles, some sourced from various international railway operators and some from the surrounding rail industry, were applied to high pressure torsion testing and the effects of different characteristics were evaluated using an ordinary least squares model.

1.2. HPT concept

High pressure torsion (HPT) rigs have become an emerging technique for studying aspects of the wheel/rail contact such as: traction behaviour [11], the impact of water and oxides on adhesion [12], & investigating the effect of surface roughness on contact stiffness [13]. The HPT method is especially suited for experiments with granular material (limited studies have previously been performed using this

* Corresponding author.
E-mail address: w.skipper@sheffield.ac.uk (W.A. Skipper).

[1] The term "adhesion" is an industry term, defined as the amount of traction present in the wheel/rail contact. The terms "adhesion" and "traction" are used interchangeably in this paper, unless specifically stated otherwise.

https://doi.org/10.1016/j.triboint.2022.108190
Received 28 September 2022; Received in revised form 2 December 2022; Accepted 17 December 2022
Available online 21 December 2022
0301-679X/© 2022 The Authors. Published by Elsevier Ltd. This is an open access article under the CC BY license (http://creativecommons.org/licenses/by/4.0/).

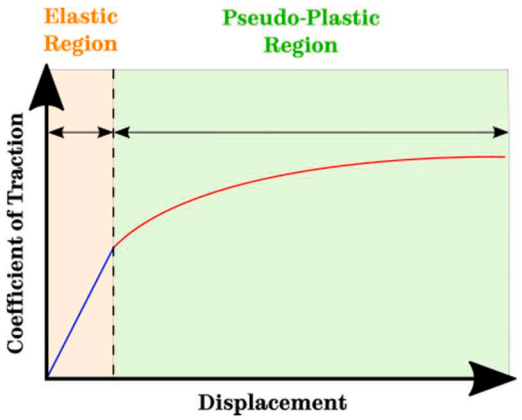

Fig. 1. Typical Example of HPT Output.

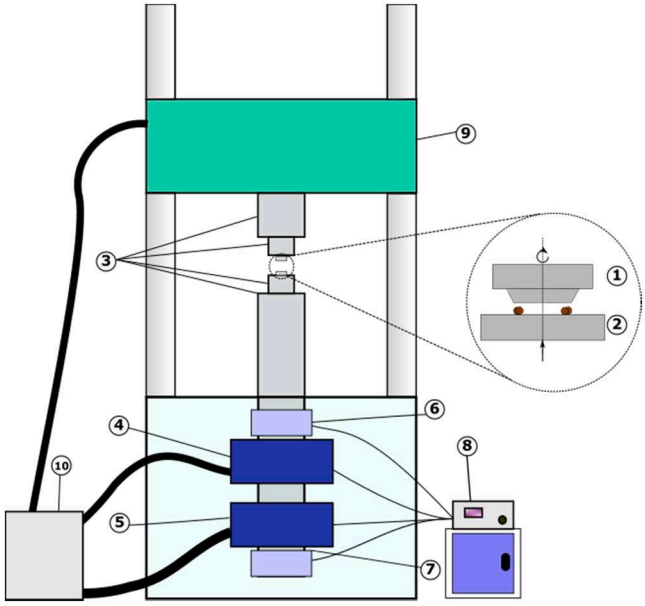

Fig. 2. Schematic of HPT Rig.

method [14,15]), as certain limiting aspects of twin-disc tests with granular material are avoided, e.g. smaller interface, recycling layers of material [16]. The HPT works by compressing two specimens together, at realistic contact pressures, and then moving a specimen through a set sweep length; the tangential stress throughout this movement is calculated and the ratio between it and normal stress is used as the measured coefficient of traction.

The typical output of a single HPT test run has been included in Fig. 1. The "elastic" region (ER) is characterised by an initial steep linear increase. The "pseudo-plastic" region (PPR) begins when asperity level contacts begin to plastically deform, work hardening the contact and leading to the coefficient of traction continuing to increase in the PPR. This asperity level plasticity was referred to as "local" or "tribological" plasticity by Six et al. [17], who also specify that this plasticity should not be confused with "global" plasticity, i.e. plastic deformation in the bulk material. For clarification: "global" plasticity can occur in the HPT contact during initial load cycles until reaching a shakedown limit, this will be discussed in further detail in later sections.

2. Methodology

In this section, the methodology surrounding the assessment of multiple particle types is presented. The particle characterisation process was used to obtain the most relevant particle characteristics for assessing their effect on tribological performance, which was evaluated using HPT testing, for which the methodology of these tests has also been presented. In addition, the methodology conducted for assessing HPT specimens' roughness is also presented here. Lastly, the ordinary least squares model used to elucidate the significance and extent of the effect of particle characteristics on tribological performance is also described.

2.1. List of particles

Particles were sourced from multiple areas: some particles were taken directly from the railway industry, some for their abrasive properties, and some for providing an extreme point of difference from typical abrasive particles i.e. lubricating particles. The list of particles that were tested included:

- Various rail sands:
  - o British rail sand (GB);
  - o Central European rail sand (CE);
  - o Derbyshire sand previously used in sanding tests (DY);
  - o Austrian rail sand (AT);
  - o Finnish rail sand (FI);
  - o Lithuanian rail sand (LT);
  - o Californian rail sand (CA);
  - o Illinoisan rail sand (IL);
  - o Japanese rail sand, no longer in use (JPD);
  - o Japanese rail sand, currently in use (JPA);
- Other particles:
  - o Aluminium oxide (AL);
  - o Diatomaceous earth (DE);
  - o Steel (NSS);
  - o Zeolite (ZL);
- Soda lime glass beads:
  - o Large glass beads, 1.75–2 mm (GL);
  - o Medium glass beads, 0.75–1 mm (GM);
  - o Small glass beads, 0.2–0.4 mm (GS);
  - o Crushed glass beads (GC).

2.2. Particle characterisation

The particle characterisation tests included in this paper are a reduced version of the particle characterisation framework described in [15]. Here, the particle characteristic tests being included are only those with relevance to their tribological performance, i.e. tests describing bulk behaviour have not been included.

2.2.1. X-Ray diffraction

X-ray diffraction (XRD) was used to discern mineral phases of each material. A Siemens D5000 X-ray powder diffraction system was utilised and scans were performed with Cu Kα1 radiation between slit angles of 5–80°. Post-processing was carried out with ICDD PDF-4 + software to identify mineral phases based on each material's respective intensity peaks.

XRD was not appropriate for all particles and some particles came with chemical consist data as part of their respective technical data sheets, so XRD has not been performed on all particles exhaustively.

2.2.2. Image analysis

The Morphologi G3S was used to carry out image analysis of each material's respective particle size and shape. Particles were dispersed onto the optical area under high pressures to ensure particle separation, and post-processing to segment each particle was performed using in-built software. Circular equivalent diameter was utilised to characterise particle size; this measurement represented the diameter of a circle with the same area as the measured particle. A representative 5–10 mm^3

Table 1
Run-in Parameters.

Parameters		Value
Contact Pressure (MPa)		900
Sweep Rate (°/s)		0.1
Oscillation End Conditions	Max Sweep Length (mm)	0.2
	Max Torque (Nm)	950
	Slip Detected	N/A
PID Loop	Proportional Term	0
	Integral Term	0.1
	Derivative Term	0

Table 2
HPT Test Parameters.

Parameter		Value
Contact Pressure		900 MPa
Sweep Length		0.4 mm
Sweep Rate		0.02 °/s
Test Progression		10°
PID Loop	Proportional Term	5
	Integral Term	0.3
	Derivative Term	0

Fig. 3. Example of Sand Placement.

of material was measured for each particle type (representative test quantities were produced using a chute splitter [18]).

Particle shape measurements were also computed at the same time. The shape parameter used in this paper was the circularity of the particle. This is defined as the ratio between the perimeter of a circle of equivalent area to the particle and the actual perimeter of the particle and takes a value between 0 and 1 with 1 denoting a circle.

2.2.3. Micro-indentation

Micro-indentation was performed using the Durascan 70 G5 with HV0.3 loading conditions. Particles were mounted in epoxy resin and subsequently ground and polished to a roughness of ~1 μm.

Three indents were made into eight particles of each material (24 indents per material). Indents that were unmeasurable were subsequently discarded, e.g. being unable to locate the indent due to local brittle fracture.

2.3. High pressure torsion testing

The high pressure torsion (HPT) rig is shown in Fig. 2, where (1) and (2) denote a top specimen (made of R8T wheel steel) and a bottom specimen (made of R260 rail steel) respectively, that when compressed together create an annulus contact; third body layers can be applied to the contact and a torque applied to the bottom specimen until it has moved through a set sweep length at a low speed (<1 mm/s). The two specimens are held in place by sample holders (3) made of 431 martensitic stainless steel. The axial position/force is controlled by a linear hydraulic actuator (5) and the actual axial position/force is measured by a linear variable differential transducer (LVDT)/load cell (7). The torsional position/force is controlled by a rotational hydraulic actuator (4) and the actual torsional position/force is measured by a rotary variable differential transducer (RVDT)/load cell (6). The attached controller (8) regulates the movement/applied force via PID loops and records both command signals and feedback signals. The crosshead (9) can be moved up and down to accommodate test apparatus between 500 mm and 2000 mm in length. The actuators are pressurised by a hydraulic ring main (10).

The wheel specimen is made of R8T steel cut directly from an actual train wheel; the contacting surface of the wheel specimen is annular with an inside diameter of 10.5 mm and an outside diameter of 18 mm. The rail specimen is made from R260 steel cut directly from an actual rail; the contacting surface is flat. The dimensions of the annular contact between these specimens were produced from an iterative method, which is fully outlined by Evans [19].

During a test run, the two specimens come into contact at an initial rate of 1 mm/s. Once contact is made, the desired normal force is applied at 20 kN/s. The test sweep is then commenced for the desired sweep length.

The procedure for a typical HPT test is thus:

1. Three run-in sequences are carried out to bring the specimen surfaces to their shakedown limit;
2. Two dry runs are performed to further run-in the surfaces and provide a dry unsanded benchmark before every test that could be used to assess whether the specimens were fully run-in. The second test start point is moved forward 10° from the previous test start point to avoid running over the same surface;
3. Any third body material is applied by hand directly to the contact patch;
4. Three test runs are performed, traction data is accrued for each test and the effect of third body materials over several runs can be deduced. Each subsequent test start point is moved forward 10° from the previous test start point to avoid running over the same surface;
5. Test specimen surfaces are analysed post-test to evaluate roughness.
6. The parameters used for run-in sequences have been included in Table 1. Tests were performed at 0°, 30°, & − 30°, with two oscillations at each angle. A “loose” PID tuning was incorporated here because this has previously been shown to effectively condition the surfaces and it was much quicker than using “tight” PID tuning.

The parameters used for HPT test runs have been included in Table 2. Unless otherwise stated, these parameters were used for all tests. It should be noted that minor changes to the test script were made to reduce the effect of stick-slip in comparison to Evans et al. [11]; a full explanation of these changes is included in [20].

2.3.1. Third body application

Particles were applied to the contact by hand, ensuring an even spread throughout the annular contact. A typical example of particle placement in dry conditions is included in Fig. 3.

For all tests with particles present in the contact, 0.025 g of material was used. This amount was selected as the sand concentration in the contact would be equal to 0.15 kg/m^2, or the maximum allowable sand concentration for British railways [21,22].

For tests conducted under wet conditions, 20 μl of distilled water was pipetted into the contact with care taken to ensure an even spread in the contact. When both water and particles were applied, the particles were applied first in the manner shown in Fig. 3 and the water was applied afterwards.

For tests conducted with a leaf layer present, 0.025 g of sycamore leaf powder was applied to the contact, ensuring an even spread. This powder was then wetted with 20 μl of distilled water using a pipette.

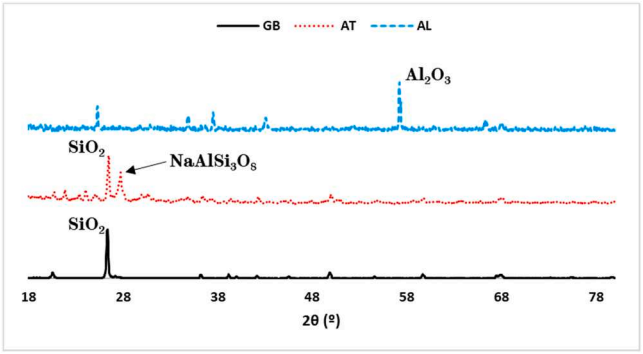

Fig. 4. XRD Analysis for Selected Particles.

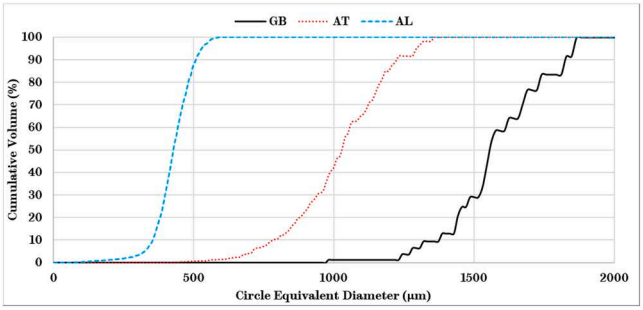

Fig. 5. Image Analysis Measurements of Circle Equivalent Diameter for Selected Particles.

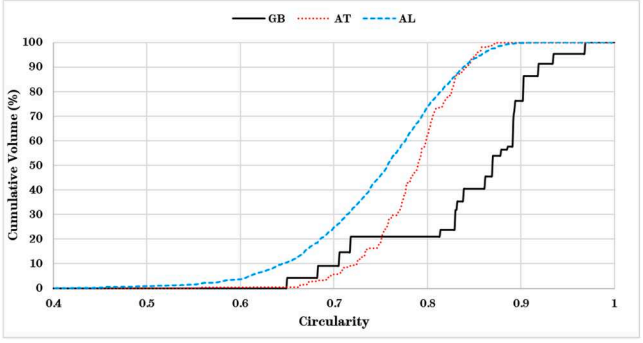

Fig. 6. Image Analysis Measurements of Circularity for Selected Particles.

One test run was then performed to condition the layer. After this conditioning run, another 20 µl of distilled water was pipetted onto the contact. For leaf tests with particles present, the particles were applied after the conditioning run and before the second application of 20 µl of distilled water. This method for creating leaf layers is different to the leaf tea method employed during previous HPT testing [15].

All particles were tested in all conditions, i.e. dry, wet, and leaf contaminated. Repeat tests were run for every test condition.

2.3.2. Post-processing of HPT data

The HPT data included in this paper were post-processed, firstly by isolating each test run, i.e. from the test start point to reaching the test finish point. The coefficient of traction was then calculated by dividing the tangential force (torque at the effective radius of friction (see Evans et al. [11])) by the axial force. Displacement was adjusted to account for a rig stiffness of 0.0005 °/Nm (see Evans for calculation [19]).

For the sake of clarity, runs under the same conditions were averaged. The traction data includes two or three runs for each condition which have been interpolated and averaged for every 0.0001 mm, and the data has been plotted with error bars denoting one standard deviation above and below every 200th data point for the sake of clarity. Unless otherwise stated the runs that are being plotted are the initial test run after surface conditioning/material application.

2.4. Post-test surface scanning

Measurements of the surface roughness of the tested specimens were taken using the Alicona InfiniteFocusSL 3D optical profilometer with some post-test analysis performed within the in-built software. At the end of all test runs, each respective wheel and rail specimen was scanned in two different locations. A 3D scan was taken covering a 3.66 mm × 3.66 mm area (vertical resolution of 500 nm) for each specimen, though it should be noted that when this was not possible (e.g. due to immovable contamination), a smaller area was used to obtain measurements. The measure of roughness used was the root mean square (RMS) height, S_q, from the reference plane of each surface (calculated from an in-built function of the software). The roughness (S_q) of the pre-test specimens was 2.46 µm for the wheel specimen and 2.40 µm for the rail specimen.

For presentation purposes, RMS height, S_q, was calculated for each set of test specimens and averaged over repeat runs, with the standard deviation included as an error bar. Where further analysis is undertaken individual measurements were used.

2.5. Ordinary least squares models

Ordinary least squares regression models were generated to assess the existence of any links between particle characteristics and performance in the HPT contact. The models took all particles previously mentioned in Section 2.1.

Before data were modelled, they were scaled according to a normal distribution, where the mean was equal to zero and unit standard deviation was used. In this way, coefficients could be more easily compared. The null hypothesis used was that the particles did not affect tribological behaviour. The models were generated using the ordinary least squares techniques contained within the Statsmodel library in Python.

3. Results

The following tests conducted as part of this paper were utilised to measure the particle characteristics and HPT performance of all particles mentioned in Section 2.1. The results from only three selected materials (GB, AT, and AL) have been shown here with all results included in Appendix A; the intention of this was to provide an example of the process that was undertaken for all tested particles as well as their potential difference, whilst maintaining clarity and brevity. The ordinary least squares models at the end of this section were generated using all tested materials, not just the selected materials shown.

3.1. Particle characterisation

The particle characterisation included in this paper includes only tests for which parameters for generating ordinary least squares models were produced. A full particle characterisation framework for assessing adhesion materials was included in a previous paper by the authors [15]. For some of the tested materials data sheets were used, where appropriate, to produce particle characteristics.

3.1.1. Mineralogy

The XRD analyses for GB, AT, and AL have been included in Fig. 4, where the constituent materials and their respective maximum intensity peaks are highlighted. Both GB and AT involved pure silica, with the latter including another silicate phase. AL was found to be pure alumina.

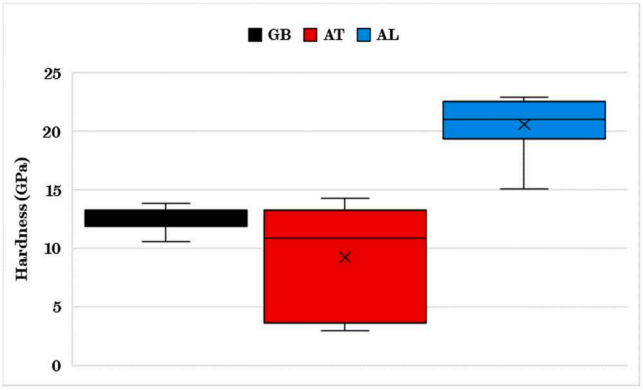

Fig. 7. Micro-Indentation Measurements of Hardness for Selected Particles.

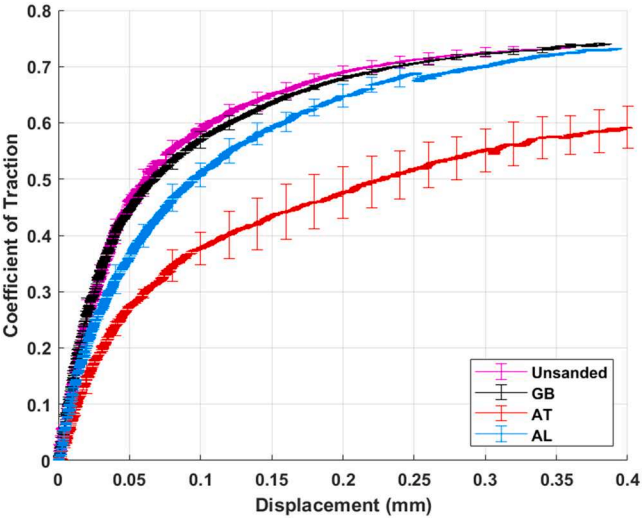

Fig. 8. HPT Traction Data for Dry Conditions with Selected Particles.

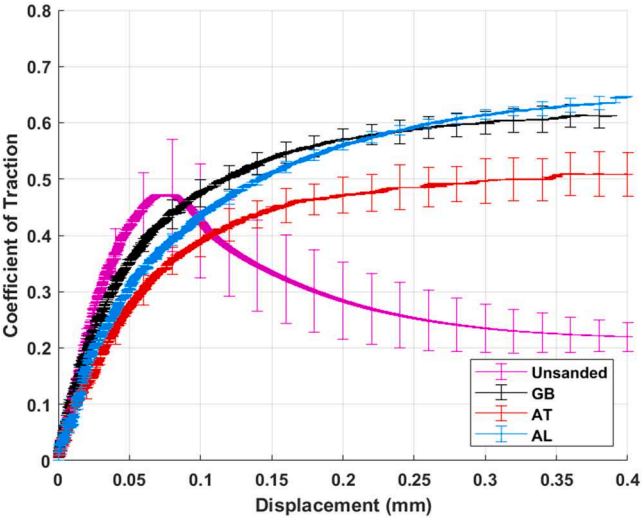

Fig. 9. HPT Traction Data for Wet Conditions with Selected Particles.

3.1.2. Particle size

Measured particle size distribution for each selected particle has been included in Fig. 5, where inferences about the typical particle size and the uniformity of sizes can be made. The selected particles range from ~300 μm up to ~1800 μm in size, this size range was typical for all tested particles.

The uniformity of selected particles also varies (inferred by the gradient of the lines). For example, GB has a relatively large spread compared to AL; this difference in uniformity was seen for all tested particles.

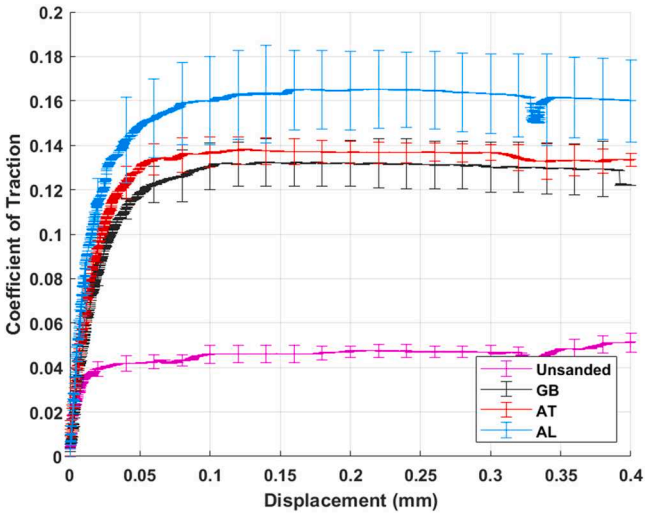

Fig. 10. HPT Traction Data for Leaf Contaminated Conditions with Selected Particles.

3.1.3. Particle shape

Measured particle shape distribution for selected particles is illustrated in Fig. 6. All the particles shown here are relatively circular in nature, being between 0.6 and 0.9. This was generally the case for all tested particles.

3.1.4. Particle hardness

Measured particle hardness has been included in the box plot forming Fig. 7. AL was the hardest particle tested. GB & AT presented hardness values that were representative of other tested sand particles, although AT produced generally lower hardness values. As hardness is an intrinsic value of the material itself, it is strongly linked to mineralogy; alumina is generally harder than silicates, and pure silicates (quartz) are stronger still than those with other constituent phases, this may explain the differences in measured hardness.

3.2. High pressure torsion testing

3.2.1. Traction data

There was a spread in the traction values measured during HPT tests conducted in dry conditions, with this spread being apparent in Fig. 8. For all traction data presented in this paper, error bars denoting one standard deviation on either side are plotted for every 200 points for the purposes of clarity. GB produced similar traction data to the unsanded case, with AL eventually producing a similar level of traction as well. AT, however, produced noticeably lower traction than the unsanded case.

In wet conditions, the coefficient of traction was reduced in all cases compared to dry conditions, as can be seen in Fig. 9. In the unsanded case, the coefficient of traction peaks at just below 0.5 before a gross slip occurs in the contact, reducing shear stress and bringing the coefficient of traction down to just above 0.2; upon gross stick-slip occurring, the variation in measured coefficient of traction for wet unsanded data also increased substantially. Similar stick-slip behaviour and traction values were observed by Buckley-Johnstone et al. [12], where it was thought that the water mixing with oxide was the root cause. This gross stick-slip was not apparent when the selected particles were applied to the contact

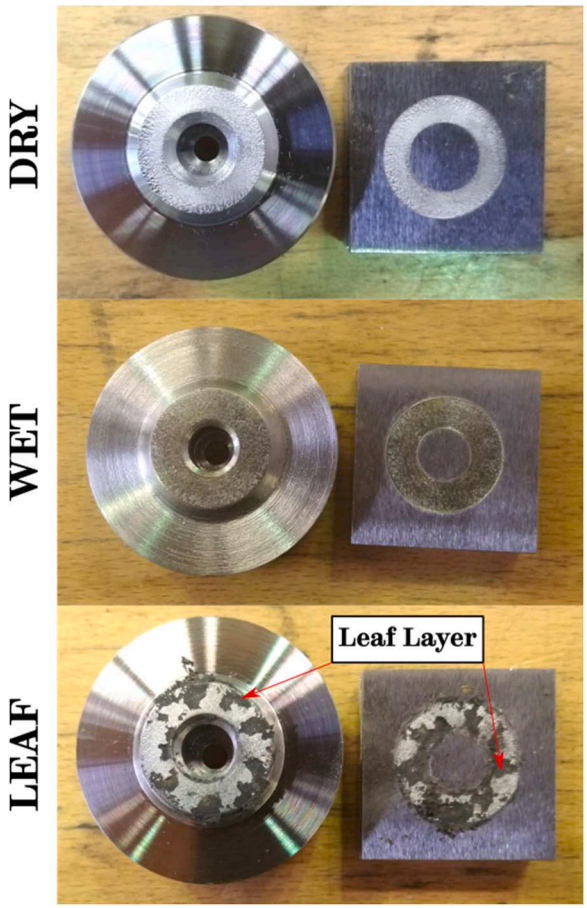

Fig. 11. HPT Specimen Surfaces after Testing conducted with No Applied Traction Enhancing Material.

(this was not the case for all tested particles). Similar to dry conditions, in wet conditions AT produced lower values of traction than both GB & AT.

In leaf contaminated conditions, coefficient of traction was markedly reduced compared to both dry and wet conditions, as can be seen in Fig. 10. In the unsanded case, peak coefficient of traction did not go above 0.05. As the minimum level of traction required for braking is 0.09 (as specified in a review by Fulford [2]), it can be considered that low adhesion is apparent in the unsanded, leaf contaminated contact. GB, AT, and AL all increased traction above 0.09 with the latter producing slightly higher traction than the former two.

3.2.2. Post-test surface analysis

Example images of the HPT contact after testing with no applied traction enhancing material are shown in Fig. 11. The dry specimens appear to be shinier than the wet specimens, possibly due to the distilled water present in the latter case more easily retaining wear debris. There is a black layer present in the leaf contaminated condition, though the visible steel underneath seems to be shinier than in the wet case.

Example images of the specimen surfaces after testing with the selected materials have been included in Fig. 12. From comparing the post-test specimens that were subjected to dry conditions, it is apparent that there is a difference between the different particle types relating to the amount of material remaining in the contact, suggesting one possible reason for the differences observed in their respective coefficients of traction. When water was applied to the HPT contact, more material appeared to remain, this is especially apparent for GB. Much of the material applied into the leaf contaminated HPT contact also remained within the contact as it embedded itself into the leaf layer, there also appears to be a difference in the amount of leaf layer remaining compared to the leaf layer shown in Fig. 11, especially when AL was applied.

The post-test surface roughness data from HPT tests conducted in dry, wet, and leaf contaminated conditions has been included in Fig. 13. Whilst comparing the average roughness values is of interest, the variation in measured values between different tests is also noteworthy, GB for example producing a very wide variance in roughness measurements. This variance in results infers the underlying probabilistic nature of single particle crushing. Generally, the specimen made of wheel steel tended to see greater roughness after testing, possibly due to being softer than the rail steel [23].

When water was applied to the contact, a reduction in roughness was observed in unsanded conditions. Similar magnitudes of roughness were observed between dry and wet conditions when traction enhancing materials were applied, with perhaps a small increase in roughness observed in wet conditions.

From the roughness measurements taken after tests conducted in leaf contaminated conditions it can be seen that similarly to wet conditions, the unsanded case saw lower measured roughness values than was observed in dry conditions. One particular material of interest from these tests is the lower amount of roughness generated by AL in these conditions; most other materials produced roughness values of a similar magnitude to the aforementioned dry and wet conditions.

Fig. 14 includes the post-test surface roughness scans taken by the Alicona. In unsanded conditions, the dry scans showed greater changes in height than both wet and leaf contaminated scans. In the leaf contaminated scans, the areas where a leaf layer was still present are noticeable due to their pronounced magnitude and sudden change in height.

The applied particles all seemed to behave differently across the contact conditions. GB made little impact in dry conditions, more in wet conditions and significantly more in leaf contaminated conditions compared to the unsanded case. AT seemed to have an impact in all conditions, though potentially slightly less in leaf conditions. AL had some impact in dry and wet conditions, though remarkably little impact in leaf contaminated conditions compared to the unsanded case. These scans seem to corroborate the data exhibited in Fig. 13.

3.3. Ordinary least squares models

The results of the HPT testing were used to fit several ordinary least squares regression models to statistically test links between particle characteristics and peak coefficient of traction or surface roughness. All particles mentioned in Section 2.1 were used to generate these models, not just the highlighted particles presented in the previous results sections. The results for all particles with respect to their respective size, shape, and hardness have been summarised in Fig. 15. The raw, tabulated data is available upon request.

Separate models were generated for dry, wet, and leaf contaminated conditions with regard to analysing the effect of particle characteristics on the peak coefficient of traction (CoT) and surface roughness as they presented non-linear differences in their respective traction behaviours. Normality of the model residuals was checked by inspection of the QQ plots which are included in Appendix B.

Table 3 summarises the coefficients between multiple particle characteristics and traction calculated by ordinary least squares models. In both dry and wet conditions both the circularity and hardness were found to be positively, and significantly correlated with the peak coefficient of traction, no significant effect with particle size was observed. It should be noted that whilst the model for dry conditions identified significant factors, the overall model was not as well fitted to the data (indicated by an R^2 value of 0.40), reducing the explanatory power of the model.

In leaf contaminated conditions significant links were identified between size (both as a linear and a quadratic term), circularity, and

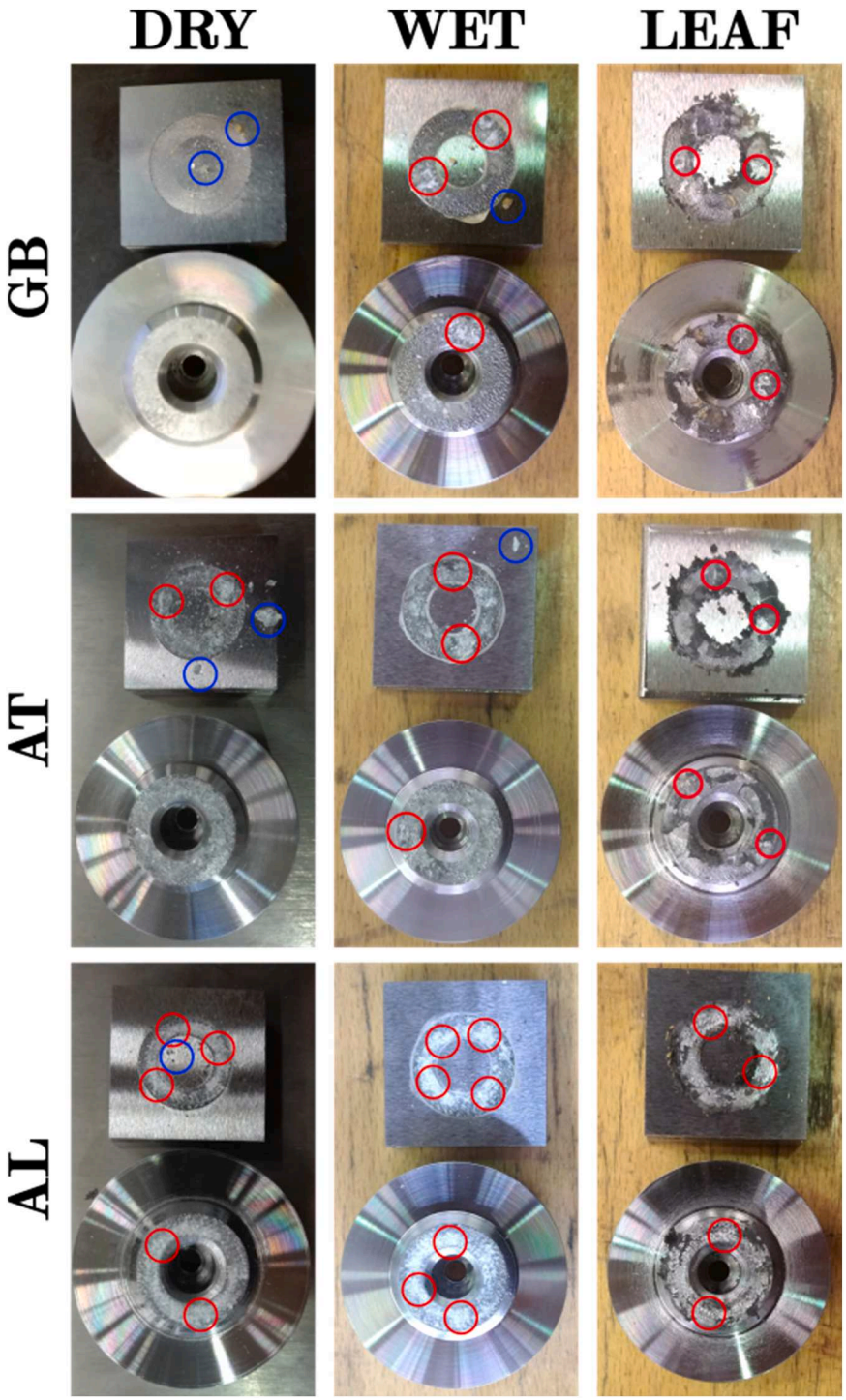

Fig. 12. HPT Test Specimen Surfaces with Remaining Material encircled in Red & Expelled Material encircled in Blue.

hardness. The existence of a link, between size and size^2 respectively, suggests that the link between particle size and traction is non-linear and that there is an ideal particle size for increasing traction in leaf contaminated conditions (similar observations were made by Arias-Cuevas et al. [24,25]). As opposed to wet and dry conditions, circularity is inversely proportional to traction, whereas the link between increasing hardness and traction was also observed in leaf contaminated conditions. Particle size had the biggest impact on traction, then hardness, and lastly circularity.

Table 4 summarises the links between particle characteristics and surface roughness of the rail and wheel specimens respectively. Compared to the models generated from coefficient of traction data (specifically the wet and leaf models), the models are not as well fitted to the data, decreasing their explanatory power.

For both the rail and wheel surfaces, both particle circularity and hardness were observed to be negatively correlated in dry conditions, whereas in wet conditions only the effect of particle circularity was found to be significant. In leaf contaminated conditions, both the rail and wheel surface roughness were positively correlated with particle size, however only the wheel surface roughness was observed to be negatively correlated with particle circularity.

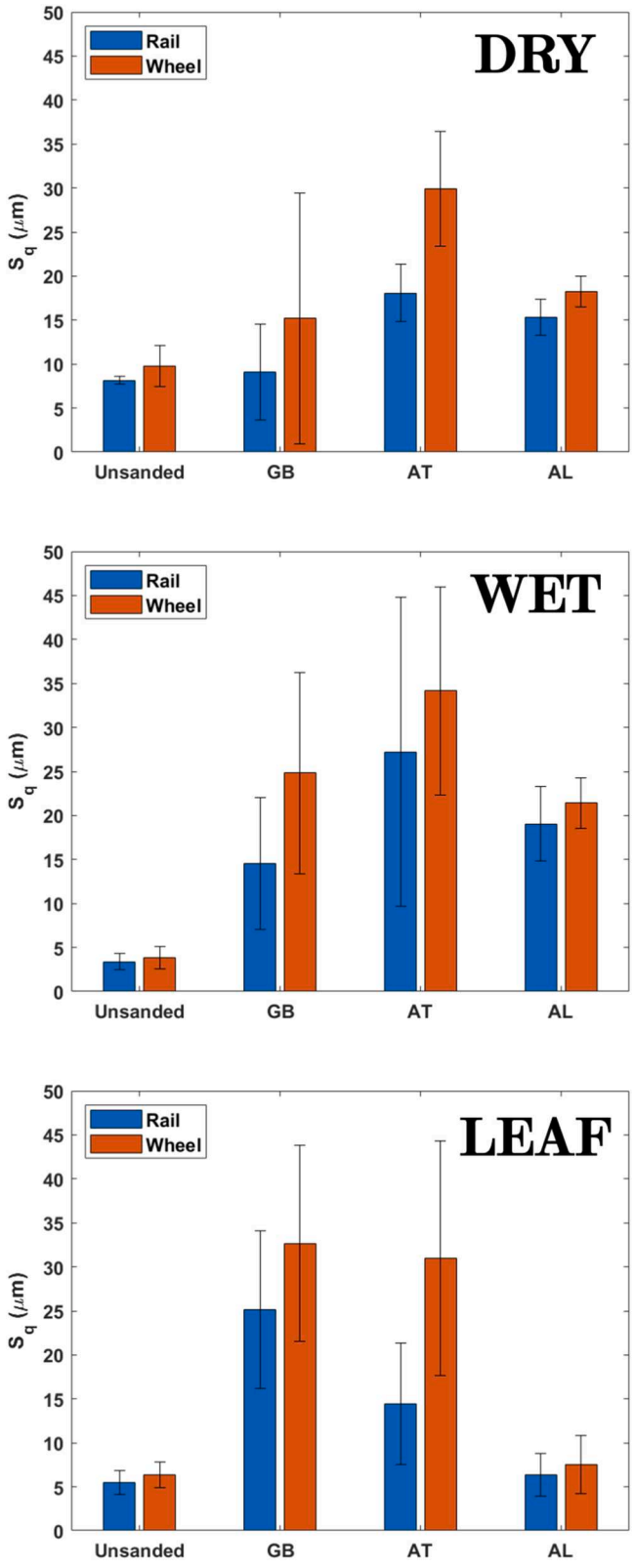

Fig. 13. Post-Test Surface Roughness Data from Dry, Wet, and Leaf Contaminated Conditions with Selected Particles.

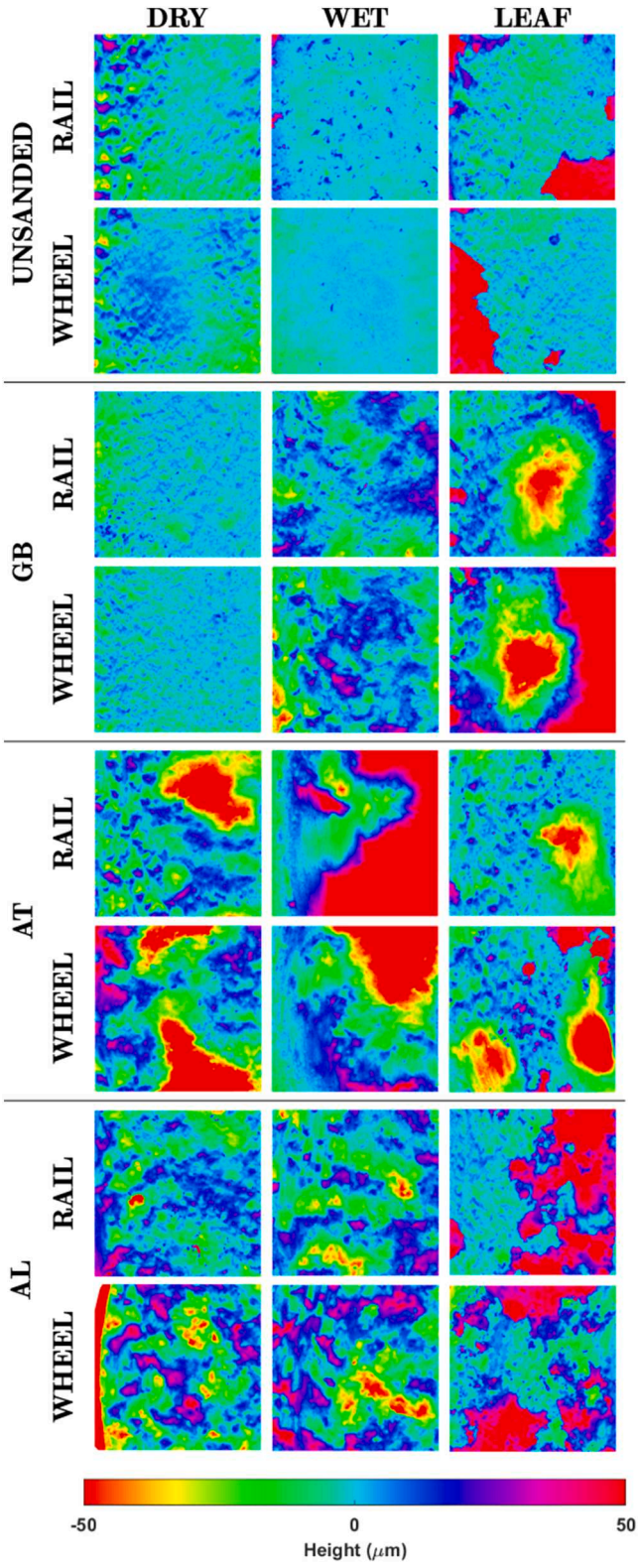

Fig. 14. Post-test Surface Scans of HPT Contacts.

4. Discussion

The following section proposes possible mechanisms for the significant trends found by the ordinary least squares models.

4.1. Expulsion of particles

In dry conditions, the amount of remaining sand seemed to play a large part in both the traction performance and the post-test surface. There did appear to be less remaining material, when compared to wet and leaf contaminated conditions, possibly due to crushed material

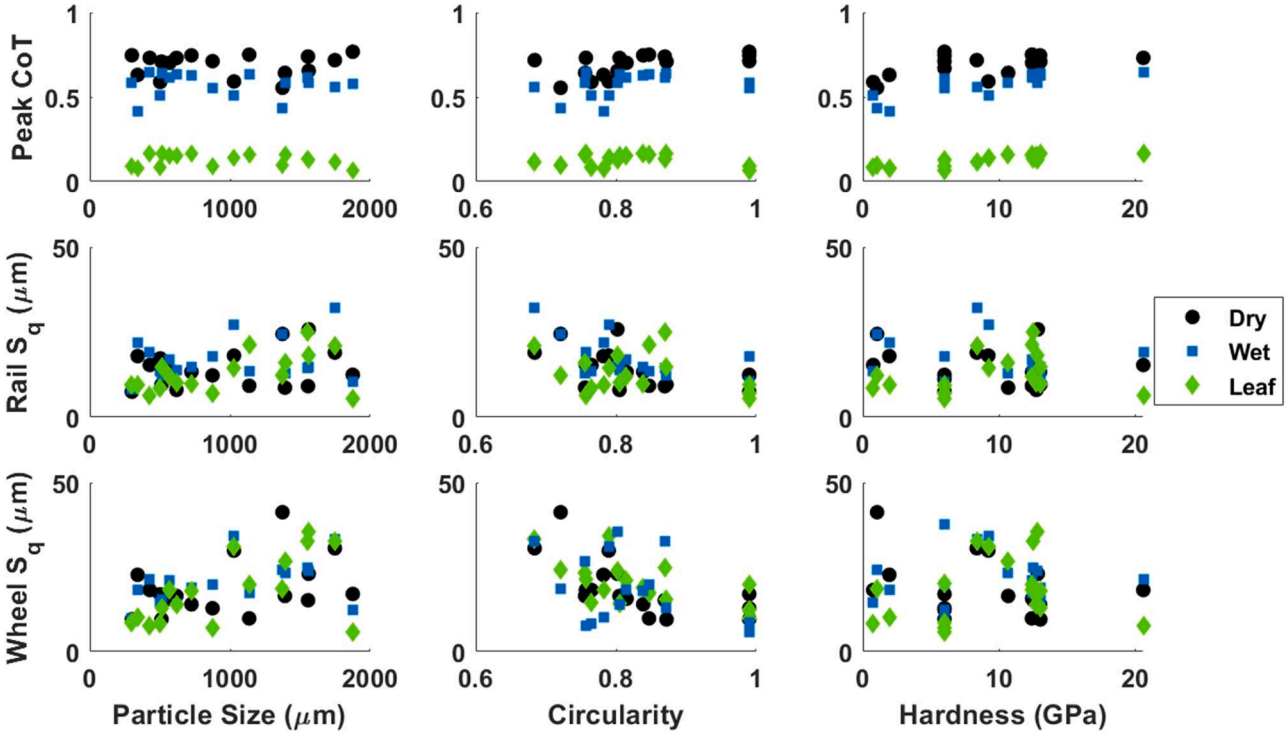

Fig. 15. Summary of Particle Characteristics vs Peak Coefficient of Traction and Surface Roughness of Rail & Wheel Specimen Surfaces Respectively.

Table 3
Summary of Variable Coefficients with respect to Peak Coefficient of Traction (Asterisks denote Statistical Significance i.e. ns= no significance/$p > 0.05$, $p < 0.05$ =*, $p < 0.01$ =**, $p < 0.001$ =***, $p < 0.0001$ =****, $p < 0.00001$ =*****).

	Dry (R^2=0.40)	Wet (R^2=0.81)	Leaf (R^2=0.84)
Size	ns	ns	1.47^{***}
Size^2	ns	ns	-1.65^{****}
Circularity	0.52^{**}	0.42^{*****}	-0.24^{***}
Hardness	0.50^{**}	0.85^{*****}	0.69^{*****}

being free to be expelled from the contact, as demonstrated in Fig. 16.

Those sands where noticeable amounts of material remained at the end of the test, also tended to exhibit lower traction data and greater surface damage. This indicates that in dry conditions remaining sand particles have the capacity to act as a dry lubricant layer, similar conclusions were arrived at from twin-disc work by Arias-Cuevas et al. [26].

In wet conditions, all sands appeared to have an amount of material remaining in the contact post-test, due to the surface tension of the water retaining particles, as represented in Fig. 16. Therefore, any differences in traction performance and surface characteristics cannot be attributed to the mere presence of rail sand alone and must be dependent on the effect of the particles when in the contact.

When material was retained in the contact, it tended to clump together; this was especially noticeable in wet conditions. This clumping in wet conditions may be due to the surface tension of the water keeping the particles more cohesive as they crush down. The inference of this is that the crushed particles retain some of their initial size, such as shown in Fig. 16.

4.2. Dry & wet conditions

It was observed that harder particles were linked with increasing traction in dry and wet conditions. As particle hardness is an intrinsic property of the material it is dependent on mineralogy. The effect of mineralogy was apparent when assessing the HPT data from the selected particles in this paper as well as from all particles (see Appendix A).

Particle hardness being such an important characteristic with regards to traction may be due to harder particles creating deeper indents between the two surfaces, transferring tractive force more effectively. A schematic of how a harder particle may behave in comparison to a softer particle has been included in Fig. 17. The harder particle is able to indent into the specimen surfaces, creating large areas against which the applied force (FA) acts, creating a couple force (FP) on the particle, which is then transferred in turn to create a reactive force (FR). This mechanism can still take place for the softer particle, however as the particle has indented less into the surfaces, it cannot transfer as much tractive force as the harder particle.

The effect of particle shape on traction in dry conditions could be explained using previous work from Nakata et al. [27]; they found that more circular particles had higher initial crushing stress. This greater initial crushing stress may result in greater stored elastic energy, thereby

Table 4
Summary of Variable Coefficients with respect to Surface Roughness (Asterisks denote Statistical Significance i.e. ns= no significance/$p > 0.05$, $p < 0.05$ =*, $p < 0.01$ =**, $p < 0.001$ =***, $p < 0.0001$ =****, $p < 0.00001$ =*****).

	Rail S_q			Wheel S_q		
	Dry (R^2=0.34)	Wet (R^2=0.27)	Leaf (R^2=0.29)	Dry (R^2=0.52)	Wet (R^2=0.28)	Leaf (R^2=0.43)
Size	ns	ns	0.39^{**}	ns	ns	0.44^{***}
Circularity	-0.51^{**}	-0.48^{**}	ns	-0.60^{****}	-0.42^{**}	-0.38^{**}
Hardness	-0.33^{*}	ns	ns	-0.38^{**}	ns	ns

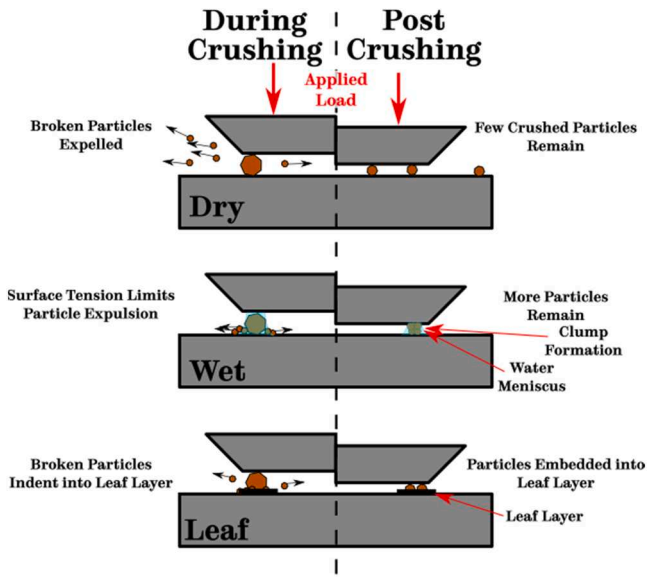

Fig. 16. Schematic of Particle Entrainment upon Crushing.

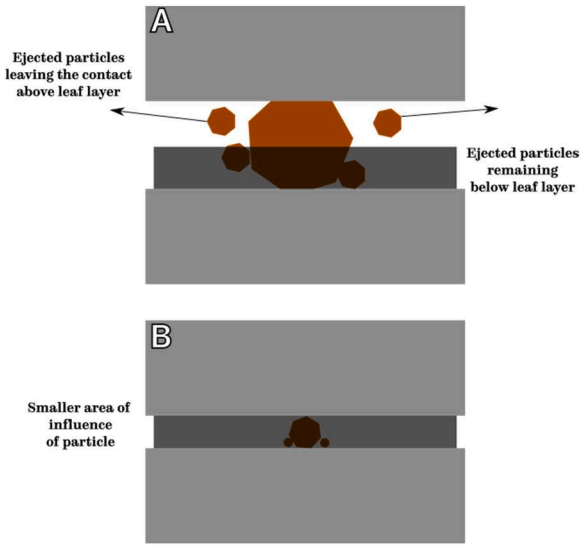

Fig. 18. Influence of Particle Size in Leaf Contaminated Contact: (a) Larger Particle; (b) Smaller Particle.

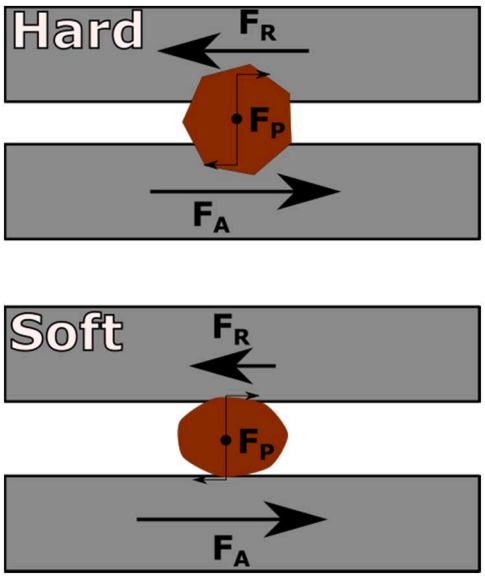

Fig. 17. Schematic of Two Particle Types in the HPT Contact: (Top) Harder Particle; (Bottom) Softer Particle.

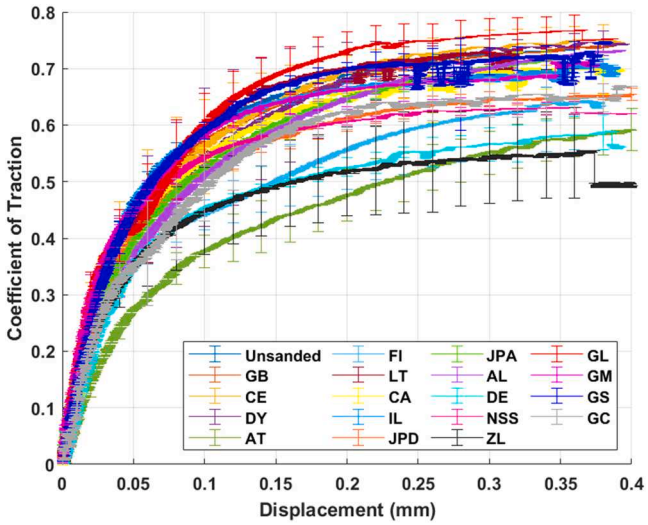

Fig. A.1. HPT Data from All Particles in Dry Conditions.

resulting in a more explosive initial fracturing of the particle, leaving less material in the contact to act as a dry lubricant. However, in wet conditions the presence of remaining material helps to provide break up the liquid lubricating layer, thus it is better for more material to be retained upon crushing. A less circular particle may break up the attractive meniscus formed by the water (see Fig. 16), leading to more material being expelled, thereby making less circular particles less effective at increasing traction in wet conditions than more circular particles.

One notable characteristic that did not have a statistically significant link with peak coefficient of traction in dry and wet conditions was particle size; it should be stressed that this does not mean that particle size did not affect traction in the HPT contact, rather no statistically significant link was observed. Previous work by Arias-Cuevas et al. [26] found there was a link between particle size and traction in dry conditions when twin-disc tests were conducted, with larger particles seeing higher traction. The proposed explanation of this was that larger particles were less easily entrained into the contact; therefore, less material was present to act as a dry lubricant.

Due to the nature of the HPT contact, the entrainment mechanism was different to a twin-disc test, this may explain the lack of a statistically significant link across all tested particles. In addition, the two test methodologies were rather different, with these twin-disc tests using a continual application of sand over many cycles. This could have led to a build-up of material on the surfaces of the discs as more material was being applied over recycled material, thus exaggerating the lubricating effect of sand application. There was, however, some evidence from glass bead tests that the largest bead size produced the highest traction.

As in dry conditions, particle size did not possess a statistically significant link with coefficient of traction. Twin-disc tests performed by Huang et al. [28] did see a link between particle size and traction in wet conditions, though the methodology differed from HPT testing, as particles were continuously applied over thousands of cycles. As noted when discussing the link between particle size and traction in dry conditions, this may have resulted in a build-up of material in the contact and a change in effect vs application at representative amounts. In addition, in their discussion of the results, it is mentioned that for the

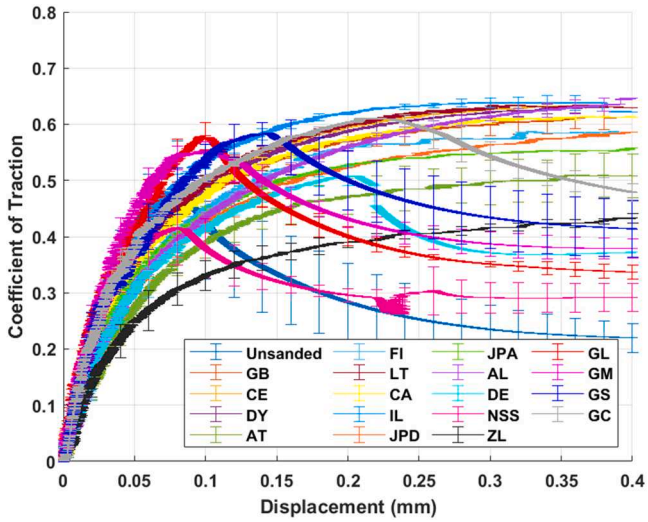

Fig. A.2. HPT Data from All Particles in Wet Conditions.

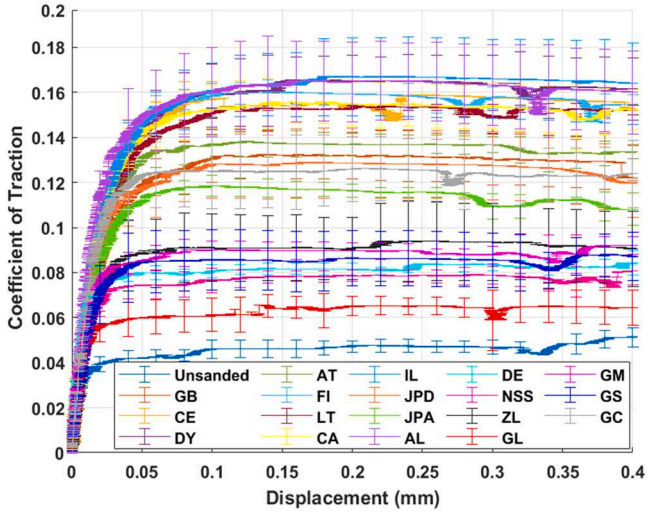

Fig. A.3. HPT Data from All Particles in Leaf Contaminated Conditions.

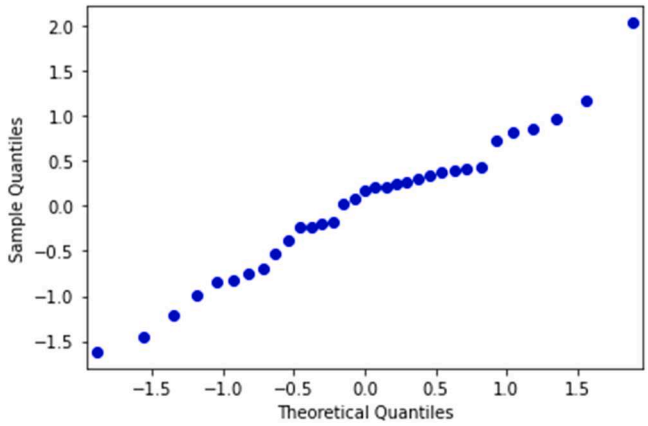

Fig. B.1. QQ Plot for Dry Model with respect to Coefficient of Traction.

"early period" (when sand first begins to be applied) "adhesion coefficient fluctuates intensely" and only after many cycles does it then become stable, suggesting the effect of particle size is not as clear when

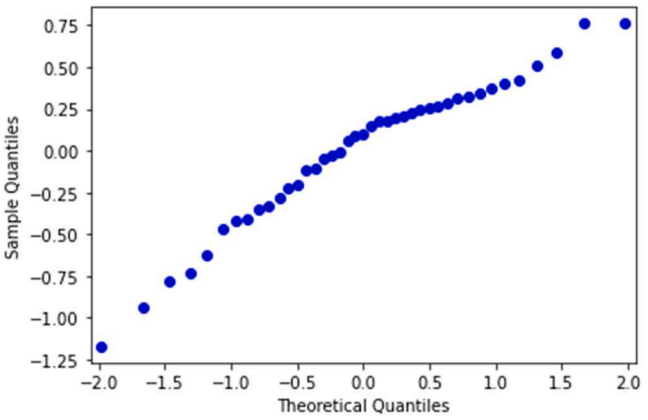

Fig. B.2. QQ Plot for Wet Model with respect to Coefficient of Traction.

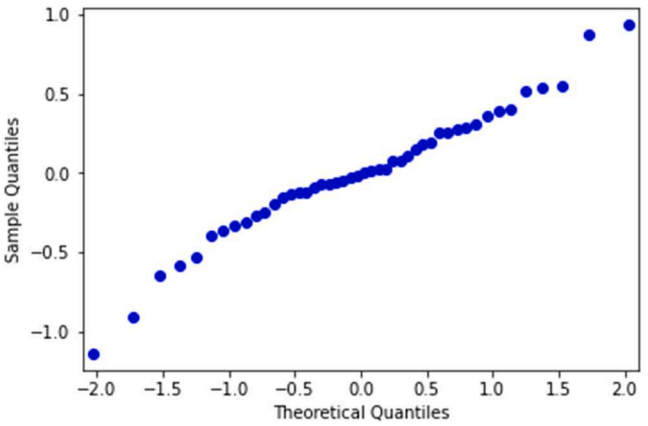

Fig. B.3. QQ Plot for Leaf Model with respect to Coefficient of Traction.

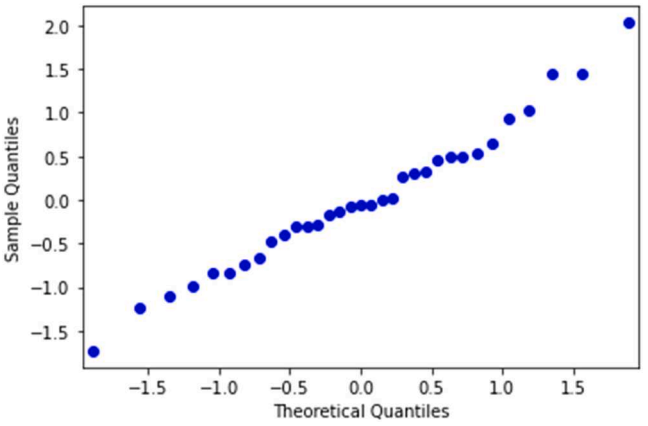

Fig. B.4. QQ Plot for Dry Model with respect to Rail S_q.

sand is being initially applied (similar to HPT testing).

4.3. Leaf contaminated conditions

When analysing leaf contaminated conditions different trends compared to dry and wet conditions were apparent. With and without soft particles (AC & NA) being included, hardness was positively correlated with peak CoT and size had significant first-order and second-order terms. When only hard particles were included these trends became stronger, and shape also became a significant factor.

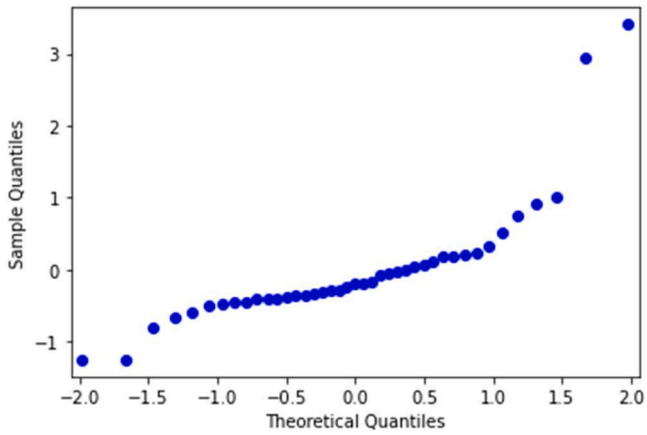

Fig. B.5. QQ Plot for Wet Model with respect to Rail S_q.

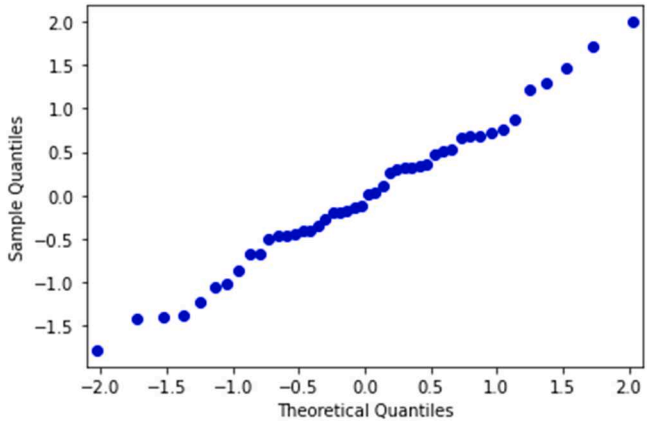

Fig. B.6. QQ Plot for Leaf Model with respect to Rail S_q.

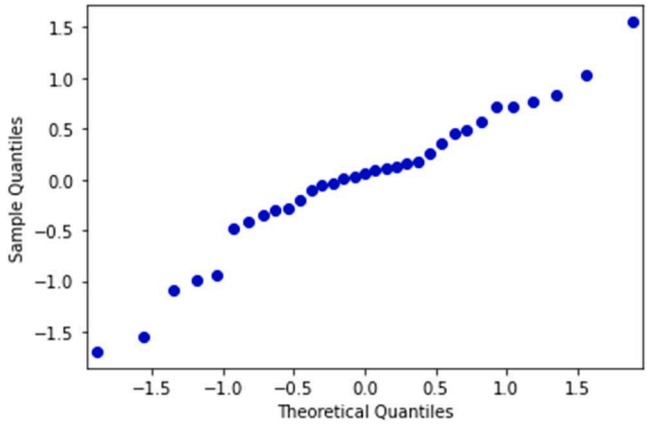

Fig. B.7. QQ Plot for Dry Model with respect to Wheel S_q.

The existence of an optimum particle size for restoring traction in leaf contaminated contacts was also observed in twin-disc and field trials conducted by Arias-Cuevas et al. [24,25]. Fig. 18 illustrates how a large particle may act upon being crushed in a leaf contaminated, HPT contact; after the particle has embedded into the leaf layer it will begin to break apart. The particle breakages occurring above the leaf layer would expel particles in a similar manner to what is seen in a dry contact, whereas breakages below the leaf layer would retain the ejected particles within the leaf layer itself. Thus, the larger the particle, the more of

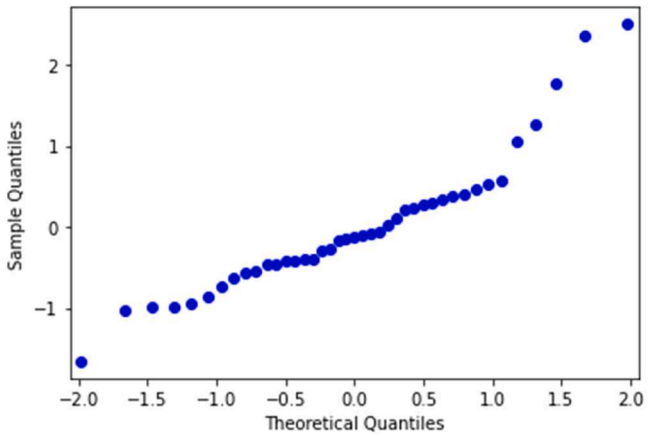

Fig. B.8. QQ Plot for Wet Model with respect to Wheel S_q.

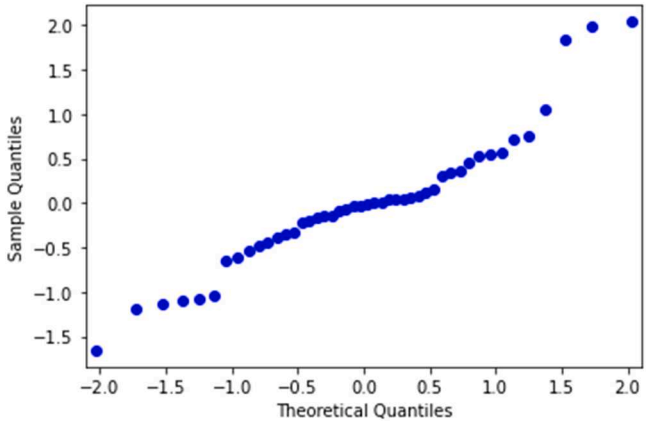

Fig. B.9. QQ Plot for Leaf Model with respect to Wheel S_q.

it will be above the leaf layer and be expelled from the contact. Fig. 18 also includes a schematic of a small particle in a leaf layer, in this case as the entire particle is embedded into the leaf layer the entire particle will act upon it. A smaller particle, however, will act over less of the leaf layer area, thus not having as great a cleaning effect on it.

The link between decreasing particle circularity and increasing traction can be explained by the less circular particle potentially being more elongated and therefore acting over a larger area of the leaf layer (in comparison to a more circular particle of the same volume). The link with hardness is probably the same mechanism as previously discussed for dry and wet conditions, though in this case, the particles' effect on the leaf layer is more important than the wheel/rail surfaces below, thus making particle hardness less important than for dry and wet conditions.

4.4. Post-test surface roughness

In all conditions, particle circularity had a statistically significant effect on surface roughness (albeit not on the surface of the rail specimen in leaf contaminated conditions). A less circular particle will correlate with being a more elongated particle, thereby creating a greater surface area between the particles and the top and bottom specimens (an elongated particle will lie on its most stable surface i.e. the largest surface).

In dry conditions, decreasing particle hardness was observed to increase surface roughness. Whilst this may seem counter-intuitive, this relationship can be explained by the link between particle strength and fracture mechanism identified by Wang and Coop [29]. They observed that particles with greater crushing strength (such as quartz) were more

likely to produce "explosive" fractures, resulting in multiple fragments with high kinetic energy being formed, by comparison, particles with lower crushing strength (such as non-pure silicates, feldspars etc.) were less likely to see this fracture mode. In the context of HPT testing, explosive fracture would make the likelihood of material remaining in the contact less likely, thus decreasing the amount of debris roughening the surface. In wet and leaf contaminated conditions, this effect may be lessened due to the factors outlined in Fig. 16.

Previously, it was theorised that harder particles may indent more deeply into the surface, increasing traction in the contact. However, this was not apparent from the links between hardness and surface roughness presented in Table 4. A possible explanation for this may be due to the differences in indentation depth between particles of different hardnesses being small, but as the relationship between indentation depth and indent surface area is non-linear, this small increase in depth can lead to a much higher surface area upon which the tractive force can act (see Fig. 17). As the measurement of surface roughness for each point was one-dimensional, only the small increase in indentation depth would be measured.

A statistically significant link between particle size and surface roughness was only observed in tests conducted in leaf contaminated conditions. The effect of increasing particle size increasing surface roughness was also observed in work undertaken by Huang et al. [28], though these tests were conducted using a twin-disc set-up in wet conditions. This relationship only being statistically significant in leaf contaminated conditions could be explained by the leaf layer retaining the structure of a particle upon crushing, with the layer physically constricting the particle; some evidence of this can be observed in Fig. 12, especially for GB. If the initial particle structure is better retained, the influence of the initial particle size will have a greater effect on the final surface roughness, much as outlined in Fig. 18 (though no non-linear relationship was identified as statistically significant with regard to surface roughness).

5. Conclusions

In this paper, the high pressure torsion (HPT) rig was adapted for testing granular material in low adhesion conditions. The HPT rig simulates the wheel/rail interface through high contact pressures and the stick-slip nature present in the contact. Numerous particle types were applied to the HPT contact in dry, wet, and leaf contaminated conditions.

For both dry and wet conditions, increasing particle hardness and circularity increased the measured peak coefficient of traction, with hardness being the stronger of the two trends. Hardness also appears to have a positive effect on peak CoT in leaf contaminated conditions, though the effect of increasing particle size is much stronger. This relationship between particle size and peak CoT is non-linear and suggests the existence of an optimum particle size for mitigating against leaf layers. Particle circularity is negatively correlated with peak CoT when leaf layers are present.

Post-test surface roughness increased with decreasing particle circularity in all tested conditions. In addition, in dry conditions, there was a statistically significant link between decreasing particle hardness and increasing surface roughness, whilst in leaf contaminated conditions the relationship between increasing particle size and surface roughness was found to be statistically significant.

These analyses suggest that harder particles are the most effective at restoring traction in low adhesion conditions (such as leaves on the line). In addition, a less circular particle is preferable and an optimum particle size for low adhesion conditions exists (though the impact on the application of the particle from the hopper up to the wheel/rail contact may temper this).

The analysis of trends regarding the effect of particle characteristics on wheel/rail traction and surface conditions will aid the selection and/or design of prospective particle types for use in railway sanding. In addition, the inferences made concerning the mechanisms by which particles restore adhesion in the wheel/rail contact can create a better understanding of the sanding process and may be used to optimise sanding products and systems.

Further work may focus on adapting the HPT method to analyse the effect of particle characteristics on wheel/rail isolation. This work would allow for a better understanding of what type of particle is most compatible with track circuits, and what possible compromises may have to be made with respect to what particle characteristics are most effective for restoring adhesion. In addition, understanding the effects of particle characteristics on particle application and entrainment into the wheel/rail contact, combined with the work in this paper, would create a more holistic understanding of the effect of particle characteristics in the sanding process.

CRediT authorship contribution statement

Roger Lewis: Supervisor; Conceptualisation; Project Administration; Writing – review and editing. Anup Chalisey: Supervisor; Writing – review and editing. Michael Watson: Investigation; Methodology; Writing – review and editing. Sadegh Nadimi: Conceptualisation; Methodology; Writing – review and editing. William Skipper: Investigation; Methodology; Writing – original draft.

The authors confirm that this is original work and the paper has not been submitted elsewhere for publication.

Declaration of Competing Interest

The authors declare the following financial interests/personal relationships which may be considered as potential competing interests: William Skipper reports financial support was provided by Engineering and Physical Sciences Research Council. Sadegh Nadimi reports financial support was provided by Engineering and Physical Sciences Research Council. Michael Watson reports financial support was provided by Engineering and Physical Sciences Research Council. Anup Chalisey reports a relationship with The Rail Safety and Standards Board that includes: employment.

Data availability

Data will be made available on request.

Acknowledgement

This work was supported by the Engineering and Physical Sciences (UK) Research Council and Rail Safety Standards Board (UK) (grant number EP/L01629X/1). The second and third authors were supported by the EPSRC (UK) (grant number EP/001766/1) as a part of 'Friction: The Tribology Enigma' Programme Grant (www.friction.org.uk), a collaboration between the Universities of Leeds and Sheffield. For the purpose of open access, the author has applied a Creative Commons Attribution (CC BY) license to any Author Accepted Manuscript version arising.

Appendix A

see Fig A.1 Fig A.2 Fig A.3.

Appendix B.

see Fig B.1 Fig B.2 Fig B.3 Fig B.4 Fig B.5 Fig B.6 Fig B.7 Fig B.8 Fig B.9.

References

[1] P. Gray, T1107 Sander Trials Dissemination Event, 2018. [Online]. Available: https://www.rssb.co.uk/Pages/adhesion.aspx.

[2] C.R. Fulford, Review of low adhesion research (T354) (RSSB Report), 2004. [Online]. Available: https://www.sparkrail.org/Lists/Records/DispForm.aspx?ID=9539.
[3] Rail Accident Investigation Branch, Autumn Adhesion Investigation Part 3: Review of adhesion-related incidents Autumn 2005 (RAIB Report), 2007.
[4] Beagley TM, Mcewen IJ, Pritchard C. Wheel/rail adhesion-boundary lubrication by oily fluids. Wear 1975;vol. 31:77–88.
[5] Beagley TM, Pritchard C. Wheel/rail adhesion - the overriding influence of water. Wear 1975;vol. 35(2):299–313.
[6] L. Buckley-Johnstone, R. Lewis, K. Six, and G. Trummer, Modelling and quantifying the influence of water on wheel/rail adhesion levels (RSSB Report), 2016. [Online]. Available: https://www.sparkrail.org/Lists/Records/DispForm.aspx?ID=24280.
[7] Ishizaka K, Lewis SR, Lewis R. The low adhesion problem due to leaf contamination in the wheel/rail contact: bonding and low adhesion mechanisms. Wear 2017;vol. 378–379:183–97.
[8] Rail Safety and Standards Board, Performance and Installation Criteria for Sanding Systems (T797), 2013.
[9] Skipper WA, Chalisey A, Lewis R. A review of railway sanding system research: adhesion restoration and leaf layer removal. Tribol - Mater Surfaces Interfaces, vol. 12; 2018. p. 237–51.
[10] Skipper WA, Chalisey A, Lewis R. A review of railway sanding system research: wheel/rail isolation, damage, and particle application. J Rail Rapid Transit, vol. 234; 2019. p. 567–83.
[11] Evans M, Skipper WA, Buckley-Johnstone L, Meierhofer A, Six K, Lewis R. The development of a high pressure torsion test methodology for simulating wheel/rail contacts. Tribol Int 2021;vol. 156(106842).
[12] Buckley-Johnstone LE, et al. Assessing the impact of small amounts of water and iron oxides on adhesion in the wheel/rail interface using High Pressure Torsion testing. Tribol Int 2019;vol. 135(October 2018):55–64.
[13] Fukagai S, Watson M, Brunskill H, Hunter A, Marshall M, Lewis R. In-situ evaluation of contact stiffness in a slip interface with different roughness conditions using ultrasound reflectometry. Proc R Soc A Math Phys Eng Sci 2021;vol. 477(2255).
[14] Meierhofer A. A new wheel-rail creep force model based on elasto-plastic third body layers. TU Graz 2015.
[15] Skipper WA, Nadimi S, Chalisey A, Lewis R. Particle characterisation of rail sands for understanding tribological behaviour. Wear, vol. 432–433; 2019.
[16] Lewis R, Dwyer-Joyce RS, Lewis J. Disc machine study of contact isolation during railway track sanding. J Rail Rapid Transit 2003;vol. 217(1):11–24.
[17] Six K, et al. Plasticity in wheel-rail contact and its implications on vehicle-track interaction. Proc Inst Mech Eng Part F J Rail Rapid Transit 2017;vol. 231(5):558–69.
[18] ASTM. ASTM C702-18: Standard Practice for Reducing Samples of Aggregate to Testing Sizep. 2018.
[19] Evans MD. Performance Assessment of Friction Management Products in the Wheel-Rail Interface. University of Sheffield; 2018.
[20] Skipper W. Sand Particle Entrainment and its Effects on the Wheel/Rail Interface. The University of Sheffield; 2021.
[21] Rail Safety and Standards Board, “GMRT2461 Sanding Equipment (Issue 3).” pp. 1–24, 2018.
[22] Lewis R, Masing J. Static wheel/rail contact isolation due to track contamination. J Rail Rapid Transit 2006;vol. 220(1):43–53.
[23] Lewis R, Dwyer-Joyce RS. Wear at the wheel/rail interface when sanding is used to increase adhesion. J Rail Rapid Transit 2006;vol. 220(1):29–41.
[24] Arias-Cuevas O, Li Z. Field investigations into the adhesion recovery in leaf-contaminated wheel–rail contacts with locomotive sanders. J Rail Rapid Transit 2011;vol. 225(5):443–56.
[25] Arias-Cuevas O, Li Z, Lewis R, Gallardo-Hernández EA. Laboratory investigation of some sanding parameters to improve the adhesion in leaf-contaminated wheel–rail contacts. J Rail Rapid Transit 2010;vol. 224(3):139–57.
[26] Arias-Cuevas O, Li Z, Lewis R. Investigating the lubricity and electrical insulation caused by sanding in dry wheel-rail contacts. Tribol Lett 2010;vol. 37(3):623–35.
[27] Nakata Y, Kato Y, Hyodo M, Hyde AFL, Murata H. One-dimensional compression behaviour of uniformly graded sand related to single particle crushing strength. Soils Found 2001;vol. 41(2):39–51.
[28] Huang W, et al. A subscale experimental investigation on the influence of sanding on adhesion and rolling contact fatigue of wheel/rail under water condition (1) J Tribol 2017;vol. 139(011401).
[29] Wang W, Coop MR. An investigation of breakage behaviour of single sand particles using a high-speed microscope camera. Geotechnique 2016;vol. 66(12):984–98.